

## Hole-LO phonon interaction in InAs/GaAs quantum dots

V. Preisler, R. Ferreira, S. Hameau, L.A. de Vaulchier, and Y. Guldner

*Laboratoire Pierre Aigrain, Ecole Normale Supérieure,  
24 rue Lhomond, 75231 Paris Cedex 05, France*

M. Sadowski

*Grenoble High Magnetic Field Laboratory, CNRS/MPI,  
25 avenue des Martyrs, 38042 Grenoble Cedex 9, France*

A. Lemaitre

*Laboratoire de Photonique et Nanostructures,  
Route de Nozay, 91460 Marcoussis, France*

(Dated: January 31, 2006)

### Abstract

We investigate the valence intraband transitions in p-doped self-assembled InAs quantum dots using far-infrared magneto-optical technique with polarized radiation. We show that a purely electronic model is unable to account for the experimental data. We calculate the coupling between the confined hole and the longitudinal optical phonons of the surrounding lattice using the Fröhlich Hamiltonian, from which we determine the polaron states as well as the energies and oscillator strengths of the valence intraband transitions. The good fit between the experiments and calculations provides strong evidence for the existence of hole-polarons and demonstrates that the intraband magneto-optical transitions occur between polaron states.

PACS numbers: 73.21.La, 71.38.k, 73.40.Kp, 78.20.Ls

## I. INTRODUCTION

Carrier-phonon interactions in quantum dots (QDs) have attracted considerable attention recently because they are essential in understanding the electronic properties of such systems, for instance the carrier relaxation which is of particular interest in QDs. Various experimental and theoretical results have demonstrated that carriers confined in InAs/GaAs QDs are strongly coupled to the longitudinal optical (LO) vibrations of the underlying semiconductor lattice<sup>1,2,3,4,5,6,7</sup>. For conduction electrons, this coupling leads to the formation of the so-called electron polarons which are the true excitations of a charged dot. Far-infrared (FIR) absorption probes directly the polaron levels instead of the purely electronic states and the electron polarons have been extensively studied by intraband magneto-optical transitions in n-doped QDs<sup>1,4</sup>. But to date, there were few investigations of valence intraband magneto-optical transitions in QDs and therefore no direct evidence for the formation of hole magneto-polarons.

In this present work, we have studied the hole excitation of p-doped self-assembled InAs/GaAs QDs using FIR magnetotransmission experiments up to 28 tesla at 2 K. We have investigated the intraband transitions between the ground and the first excited valence states. Depending on the FIR polarization, two different transitions can be excited, whose intensity and dispersion versus magnetic field show strong deviation with respect to the predictions of a purely electronic level model. Using the Fröhlich Hamiltonian, we have calculated the coupling between the low-lying confined hole states, which we find using a simple one-band model, and the lattice modes. We have determined the hole polaron states as well as the energies and oscillator strengths of the intraband transitions. We show in this work that our model fits the experimental data very well, demonstrating that the measured transitions occur between hole polaron states.

## II. EXPERIMENTAL DETAILS

The InAs/GaAs dots investigated here were grown on (001) GaAs substrates by molecular-beam epitaxy using the Stranski-Krastanov growth mode of InAs on GaAs<sup>8</sup>. As the resonant FIR absorption associated with a single dot layer is weak (a few 0.1%)<sup>1,9</sup>, samples containing a multistack of 20 layers of InAs QDs were prepared in order to strengthen this absorption. Each dot layer is separated by a 50-nm-thick GaAs barrier. The density of QDs is  $\sim 4 \times 10^{10} \text{ cm}^{-2}$  for each plane, corresponding to an average center to center distance of 50 nm, large enough to neglect any

interdot interactions. We can, therefore, reasonably consider our samples as consisting of isolated QDs. The gaps of the QDs were measured in the different samples by photoluminescence (PL) experiments at 4 K. The PL peak is centered at  $\sim 1.2$  meV, which is a typical value for lenslike InAs islands with a height of  $\sim 2$ -3 nm and a lateral diameter of  $\sim 20$  nm. The dot filling is realized by a Be delta doping of each GaAs barrier at 2 nm under each dot layer. In the following we discuss results obtained from two samples labelled (I) and (II). Sample (I) has a doping level of  $\sim 5 \times 10^{10} \text{ cm}^{-2}$ , whereas sample (II) has a doping level of  $\sim 10 \times 10^{10} \text{ cm}^{-2}$ . The doping level was adjusted to transfer on average one or two holes per dot and populate only the ground state. We have investigated the optical transitions between the ground state and first excited states. Such transitions, which involve only valence-band states, correspond to resonance energy in the FIR. The sample transmission at 2 K was recorded by Fourier-transform spectroscopy in the FIR range ( $50 - 700 \text{ cm}^{-1}$ ). In order to eliminate optical setup effects, the sample transmission was normalized to the substrate transmission. Two types of magnetotransmission experiments have been performed with the radiation propagating perpendicular to the QD layers of the samples: measurements up to  $B=15$  T using a superconducting magnet with linearly polarized light and measurements up to  $B=28$  T at the Grenoble High Magnetic Field Laboratory using a resistive magnet and non-polarized light. The magnetic field was applied parallel to the growth axis (Faraday configuration).

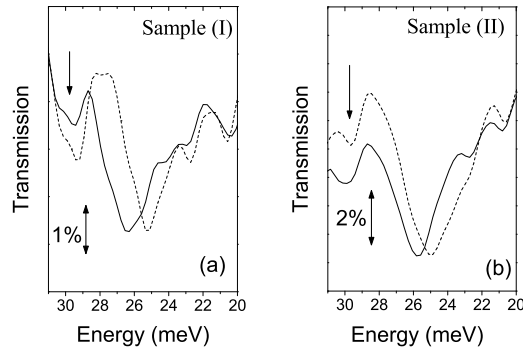


FIG. 1: Transmission spectra at  $B=0$  for radiation linearly polarized along the  $[110]$  (solid curve) and the  $[1\bar{1}0]$  (dashed curve) directions for sample (I) (a) and sample (II) (b). The arrows indicate the absorption associated with the LO-phonon of InAs.

### III. RESULTS

Intraband transitions in InAs/GaAs self-assembled QDs usually display anisotropic behavior when the FIR radiation is polarized along either the  $[110]$  or the  $[1\bar{1}0]$  direction<sup>1</sup>. Such behavior could arise, e.g., from an anisotropy of the dot shape<sup>9,10</sup>, interband and piezoelectric coupling<sup>11</sup>, or atomistic contributions<sup>12</sup>. We have therefore performed magnetotransmission spectra for FIR radiation, linearly polarized along the  $[110]$  and  $[1\bar{1}0]$  directions of the sample. Fig. 1 displays the FIR absorption spectra at zero magnetic field recorded for the two polarizations in sample (I) (Fig. 1(a)) and sample (II) (Fig. 1(b)). A main absorption is observed at an energy of  $\sim 26$  meV in both samples for the  $[110]$  polarization. For the  $[1\bar{1}0]$  polarization, the main absorption occurs at a slightly lower energy. The anisotropy related energy splitting is found to be  $\sim 1.2$  meV in sample (I) and  $\sim 0.8$  meV in sample (II). Such values are significantly less than those measured for intraband transitions in n-type samples grown in similar conditions. The sharpness of the lines [the full width at half maximum (FWHM) is  $\sim 3$  meV] is good evidence of the high quality of these samples. The main line intensity is  $\sim 2\%$  for sample (I) and  $\sim 4\%$  for sample (II). Such a difference in intensity can be explained by the different doping levels of the two samples, as described for instance in Appendix A of reference 1. Note, as well, that a smaller absorption is observed in both samples at around 29 meV (indicated by the arrows in Fig. 1). We have verified that this absorption is also measured in undoped samples grown in similar conditions, while the other absorptions associated with the doped dots are not observed. We thus associate this  $\sim 1\%$  sharp absorption with the InAs like LO phonon. Fig. 2(a) displays the magnetotransmission spectra for radiation along the  $[110]$  direction of sample (II) and recorded at 2 K from  $B=0$  to  $B=15$  T every 3 T. As the magnetic field increases, the main absorption observed at zero magnetic field at  $\sim 26$  meV stays nearly constant in energy all the while decreasing in intensity. At around 6 tesla, a second lower energy absorption appears at 23 meV. This second absorption decreases in energy as the magnetic field is increased. The zero transmission region from 32 meV to 37 meV corresponds to the reststrahlen band of the GaAs substrate.

Let us now compare this behavior with the magnetotransmission spectra for radiation polarized along the  $[1\bar{1}0]$  direction. Fig. 2(b) displays the magnetotransmission spectra for radiation polarized along the  $[1\bar{1}0]$  direction with an applied magnetic field. The absorption minimum decreases in energy as the magnetic field increases while its oscillator strength stays strong for all magnetic fields.

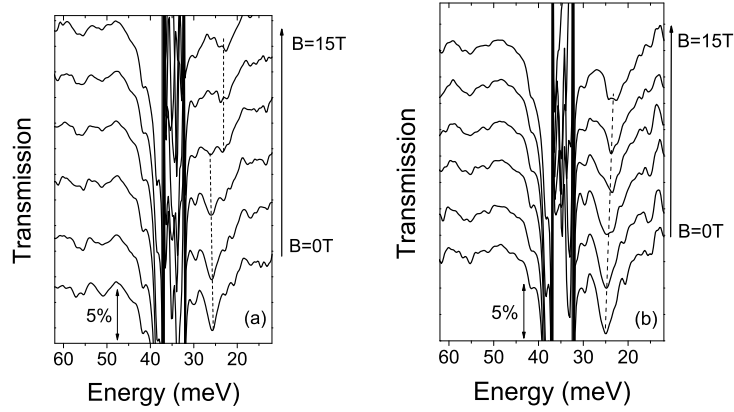


FIG. 2: Magnetotransmission spectra measured in sample (II) for radiation linearly polarized along the (a)  $[110]$  and (b)  $[1\bar{1}0]$  directions and recorded at 2 K from  $B=0$  to  $B=15$  T every 3 T. Traces have been vertically offset for clarity.

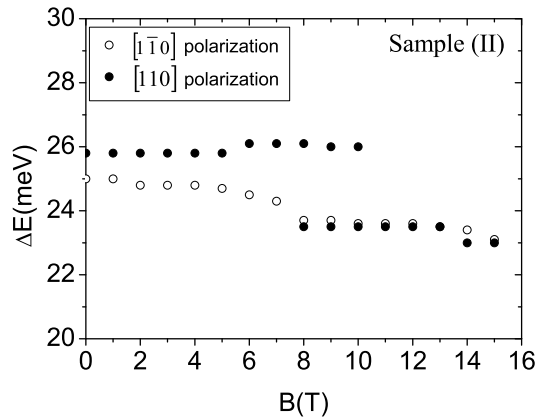


FIG. 3: Magnetic field dispersion of the resonances in sample (II) for the two polarization directions;  $[110]$  in full circles and  $[1\bar{1}0]$  in open circles.

The different behavior between these two polarizations is clearly demonstrated in Fig. 3 where we have plotted the energy absorption minima of the two polarizations as a function of magnetic field. We see that one polarization contains one unique absorption that decreases in energy while the other polarization has two absorptions: a high energy branch observable at low magnetic field and low energy branch observable at high magnetic fields. It is clear that the transition energies we observe experimentally cannot be accounted for by a simple Zeeman splitting effect that we would

expect in a purely electronic model. Indeed, the lower and upper branches would be symmetric in that case with similar oscillator strengths. We observe quite similar magnetotransmission results for sample (I).

#### IV. ANALYSIS AND DISCUSSION

In polar semiconductors, such as III-V materials, anomalies observed for intraband transitions often originate in carrier-LO phonon interactions when the energy separation between the ground and excited states approaches the LO phonon energy  $\hbar\omega_{LO}$ . The energy of LO phonons in bulk InAs is  $\hbar\omega_{LO} = 29$  meV which is very close to that of the upper branch (Fig. 3). As mentioned above, a significant absorption, that is independent of the magnetic field, is observed around 29 meV in the FIR spectra of all our samples. Because a purely electronic level model is unable to explain the experimental data, we have to consider FIR magneto-optical transitions between polaron states and, therefore, to calculate the coupling between the relevant mixed hole-phonon states. In bulk materials, it is well-known that one has to diagonalize the Fröhlich Hamiltonian that describes the Coulomb interaction between a moving charge and the dipoles vibrating at the angular frequency  $\omega_{LO}$  corresponding to a longitudinal optical mode. This mode is associated with the partial ionicity of the bonds between the two different atoms that constitute the III-V semiconductors. In QDs, the phonon spectra are not known accurately as a result of the uncertainties of the shape and composition of the actual dots. But since an actual InAs island consists of several thousand unit cells we can expect the dot to have a quasibulk phonon spectra. In addition, like in III-V bulk, each anion is surrounded by four cations with a slightly polar bond between them. Therefore, the basic ingredients of the Fröhlich Hamiltonian are maintained in actual dots. These considerations, along with the fact that it works very well for n-doped samples<sup>1</sup>, have led us to take a bulklike Fröhlich Hamiltonian to describe the interaction between a hole bound to a dot and the optical phonon mode of the structure.

We evaluate the hole states within a one-band (parabolic) model. Such a model gives an accurate description of the coupling between electrons and phonon modes in n-doped samples<sup>1</sup>. However, the use of such a simple model is less evident for the valence levels of semiconductor nanostructures, as discussed in many works (see e.g. references 11,12 and references there in). For instance, non-parabolicity and mass anisotropy should play an important role in the description of the hole states. In order to account for these effects in a simplified way, we consider an

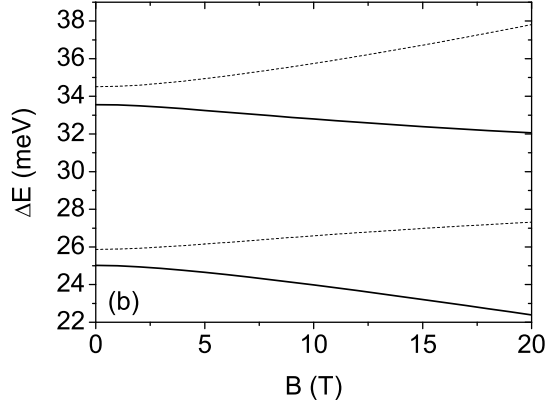
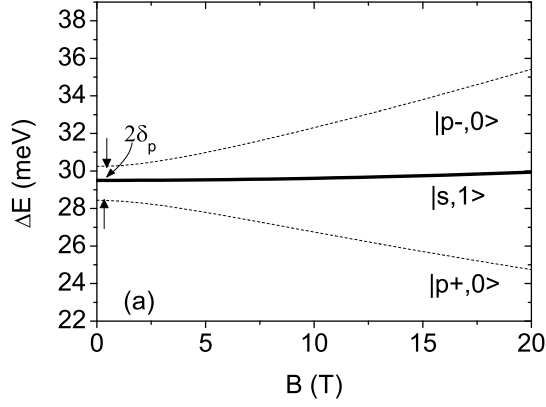


FIG. 4: Resonance dispersions calculated from the numerical diagonalization of the Hamiltonian without coupling term (a) and with Fröhlich term (b) for the parameters listed in the text.

anisotropic dispersion for heavy holes, with an in-plane mass chosen to best fit the magneto-optical experimental results. Of course, a more rigorous theory should incorporate such mass effects from the onset. However, as shown below, our model suffices to provide a good description of our experimental results using reasonable fitting parameters.

For QDs with a perfect cylindrical symmetry the ground and first excited states are  $s$ -like and  $p$ -like, respectively. By using a variational procedure with Gaussian functions<sup>13</sup>, we have calculated the energy levels of holes in a QD modelled by a truncated cone of height  $h$  and with a circular basis of radius  $R$  and basis angle  $30^\circ$  as estimated from transmission electron micrographs. We have considered a homogeneous gallium content of 30% in the QDs, resulting in a valence band

offset of 217 meV<sup>1</sup> and added an anisotropy term in order to account for the zero field splitting we observe experimentally. The noninteracting mixed hole-phonon states in an uncoupled system are labelled  $|v, n_{\mathbf{q}}\rangle$  where  $|v\rangle = |s\rangle, |p_{\pm}\rangle$  are purely electronic levels (in what follows  $p_{\pm}$  denotes the two electronic levels that result from the two excited states admixed by the anisotropy term).  $|n_{\mathbf{q}}\rangle$  denotes the ensemble of the  $n$  LO-phonon states in the  $\{\mathbf{q}\}$  modes. In Fig. 4(a) we present the calculated energy transitions for the uncoupled system, where the zero energy has been taken at the ground state ( $|s, 0\rangle$ ) energy. The splitting,  $2\delta_p$ , between the two  $p$ -like components at zero magnetic field arises from the anisotropy term. The parameters used in this calculation are described below.

Now we add the Fröhlich Hamiltonian term which couples states that differ by one phonon. As discussed in Appendix A, the numerical diagonalization of the Hamiltonian including the Fröhlich term gives the polaron states. We have taken the dimensionless Fröhlich constant  $\alpha$  that characterizes the ionicity of the material and the intensity of the coupling as an adjustable parameter. It has previously been reported that  $\alpha$  could be enhanced in dots as compared to the bulk situation<sup>14</sup>. Fig. 4(b) displays the calculated polaron levels. We observe four energy transitions: two transitions represented by dashed lines that are mainly a result of an interaction between the  $|s, 1\rangle$  continuum and the  $|p-, 0\rangle$  state and two transitions represented by solid lines that are mainly the result of an interaction between the  $|s, 1\rangle$  continuum and  $|p+, 0\rangle$  state (see Appendix A for more details).

Let us now compare our calculated polaron levels with our experimental data. The solid and dashed curves of Fig. 5 are the resonance dispersion calculated for  $\alpha = 0.13, m^* = 0.22m_0$  and the anisotropy term  $\delta_p = 0.9$  meV. A dot with a height  $h=25.4$  Å and radius  $R=91$  Å was used for this fit (Note that these parameters are also used in the calculations shown in Fig. 4(a) and Fig. 4(b)). A similar value of the Fröhlich constant,  $\alpha$ , has been determined in n-doped QDs<sup>4</sup>. The energy positions versus field are very well described by our model. The two higher energy polarons branches, predicted in Fig. 4(b), are not observed experimentally in this field range because their energies coincide with that of the restrahten band of the GaAs substrate, (grey area in Fig. 5).

In order to explain the variation in intensity we observe experimentally, we have calculated the oscillator strengths of the optical transitions between polaron levels as a function of magnetic field (Fig. 6). The equations used in these calculations are given at the end of Appendix A. The solid curves represent the evolution of the oscillator strength of the lower energy branch (labelled (1) in

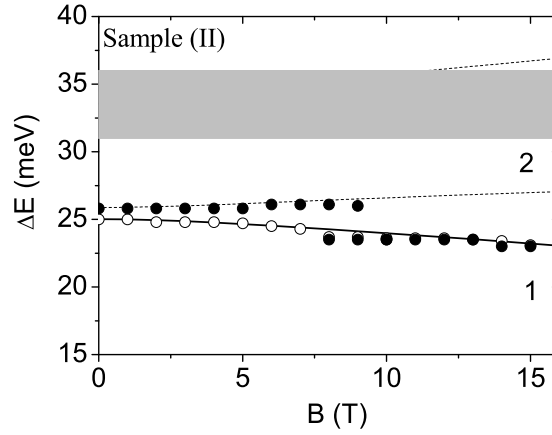


FIG. 5: Magnetic field dispersion of the resonances observed for sample(II) for the two polarization directions;  $[110]$  in full circles and  $[1\bar{1}0]$  in open circles, with the calculated energy transitions in bold and dashed curves. The grey area between 32 meV and 36 meV represented the zero transmission region of the substrate.

Fig. 5) whereas the dashed curves represents the evolution of the higher energy branch (labelled (2) in Fig. 5). In addition, the full circles correspond to light polarized along the  $[110]$  direction and the open circles to a polarization along the  $[1\bar{1}0]$  direction. Note that, at zero magnetic field, the  $\sim 4\%$  absorption measured in sample (II) for light polarized along the  $[1\bar{1}0]$  direction (Fig. 1(b)), corresponds to an oscillator strength of  $\sim 0.6$ . This is corroborated by the  $\sim 3\%$  absorption for light polarized along the  $[110]$  direction which corresponds to an oscillator strength of  $\sim 0.45$ . Taking into account the signal to noise ratio, which allows the detection of  $\sim 1\%$  transmission variation, our experimental sensitivity corresponds roughly to an oscillator strength of  $\sim 0.15$ . At zero tesla, our model predicts the existence of the higher energy branch for the  $[110]$  polarization and the lower energy branch for the  $[1\bar{1}0]$  polarization. As the magnetic field is increased, the oscillator strength of the high energy branch decreases towards the experimental limit 0.15. On the contrary, the oscillator strength of the lower energy branch increases above the experimentally observable intensity around 6 T. For the other polarization  $[1\bar{1}0]$ , our model predicts one unique observable absorption with an oscillator strength that stays nearly constant with the changing magnetic field. This is a good description of the oscillator strength behavior we observe in the magnetotransmission spectra of our samples. In addition, we note that a purely electronic model cannot predict the variation in oscillator strength with the magnetic field that we

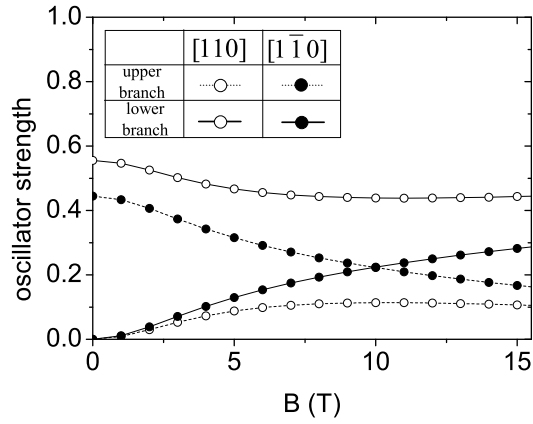


FIG. 6: Calculated magnetic field dependence of the oscillator strength for the high energy polaron (dashed line) and the low energy polaron (solid line) for light polarized along the [110] (full circles) and [1 $\bar{1}$ 0](open circles) directions.

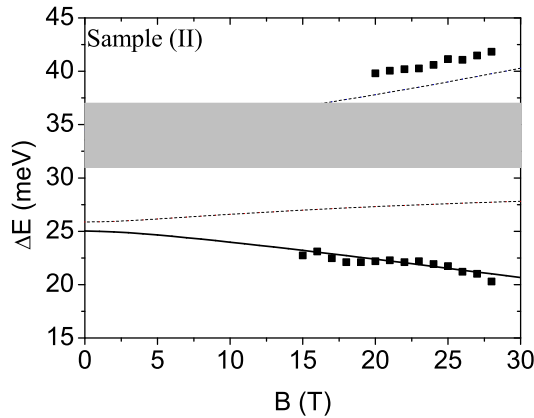


FIG. 7: High magnetic-field dispersion of the resonances (full squares) in unpolarized light for sample (II). The lines are the resonance dispersions calculated using the parameters listed in the text.

observe experimentally. The good agreement obtained for the energy transitions as well as for the evolution of oscillator strengths demonstrates that the magneto-optical transitions occur between polaron states.

Finally, we present the results of magnetotransmission measurements done on sample (II) at the High Magnetic Field Laboratory in Grenoble . In Fig. 7 we display the magnetic-field dispersion of

resonances between 15 and 28 T for unpolarized radiation. The lines are the calculated dispersions using the same parameters as above, but now calculated up to  $B=30$  T. The most important result from these additional high magnetic field experiments is that they have permitted us to experimentally observe the polaron transition at energies above the reststrahlen band of the substrate. Indeed at 20 T, we start to see an absorption at  $\sim 40$  meV. This is a significant result because this energy transition cannot be predicted using a purely electronic model. We therefore have additional experimental support that the energy transitions occur between polaron states. Note that in Fig. 7 the calculated upper branch is found to be  $\sim 2$  meV below the experimental points. Such a discrepancy could, e.g., arise from an interaction involving the LO-phonon of GaAs ( $\sim 36$  meV) which is not included in our calculations where only the InAs like LO-phonon is taken into account.

## V. CONCLUSION

In summary, we have investigated the valence intraband transitions in p-doped self-assembled InAs QDs by using FIR magneto-optical technique with linearly polarized radiation. We have shown that a purely electronic model is unable to account for the experimental data, neither for the energy dispersion of the magneto absorption resonance, nor for the intensity dependence versus magnetic field. As the transition energies are close to that of the LO-phonon in InAs, we have shown that a model taking into account the hole LO-phonon coupling is able to predict well the experimental data. We have calculated the coupling between the relevant mixed hole-lattice states using the Fröhlich Hamiltonian and we have determined the polaron states as well the oscillator strength of the polaron transitions as a function of magnetic field. We believe that the fact that our model successfully fits the experimental data constitutes the first evidence for the existence of hole polarons in InAs QDs and demonstrates that the intraband magneto-optical transitions occur between hole polaron states.

### Acknowledgments

The Laboratoire Pierre Aigrain is a mixed Research Unit (UMR 8551) between Ecole Normale Supérieure, the University Pierre et Marie Curie (Paris6) and the CNRS. We would like to thank G. Bastard for very valuable and fruitful discussions.

## APPENDIX A: CALCULATING POLARON LEVELS

In order to understand the experimental results observed in Fig. 3, we develop a simple model that involves dispersionless LO phonons. We deal with the zero-phonon discrete hole levels  $|p+, 0\rangle$ , and  $|p-, 0\rangle$  and the flat one-phonon continuum  $|s, 1\rangle$ , as well as the states  $|s, 0\rangle$ ,  $|s, 2\rangle$  and  $|p\pm, 1\rangle$  which are treated solely in perturbation. The Fröhlich term of the Hamiltonian is written as follows,

$$H_{int} = \sum_{\mathbf{q}} [V(\mathbf{q})a_{\mathbf{q}}^{\dagger} + V^*(\mathbf{q})a_{\mathbf{q}}], \quad (\text{A1})$$

where  $\mathbf{q}$  are the different modes of the LO-phonon and  $V(\mathbf{q})$  includes in its definition the dimensionless Fröhlich constant  $\alpha$ . First, we consider the interaction between one discrete level, say  $|p-, 0\rangle$ , and the one phonon continuum  $|s, 1\rangle$ . We note  $V_{sp-}(\mathbf{q}) = \langle s, 1_{\mathbf{q}} | H_{int} | p-, 0 \rangle$ . We perform linear combinations of the degenerate one-phonon states  $|1_{\mathbf{q}}\rangle$  and introduce a particular linear combination,

$$|1_{\alpha(sp-)}\rangle = \frac{\sum_{\mathbf{q}} V_{sp-}(\mathbf{q}) |1_{\mathbf{q}}\rangle}{\sqrt{\sum_{\mathbf{q}} |V_{sp-}(\mathbf{q})|^2}}, \quad (\text{A2})$$

$$\langle s, 1_{\alpha(sp-)} | H_{int} | p-, 0 \rangle = \sqrt{\sum_{\mathbf{q}} |V_{sp-}(\mathbf{q})|^2} = v_{eff}(sp-). \quad (\text{A3})$$

We label  $|1_{\beta}\rangle$  the remaining one-phonon combinations orthogonal to  $|1_{\alpha(sp-)}\rangle$ . Thus, the continuum levels  $|s, 1_{\beta}\rangle$  are uncoupled to  $|p-, 0\rangle$ . We have in this way an interaction between two discrete levels that gives rise to two polaron states. These polarons are a mixture of  $|p-, 0\rangle$  and  $|s, 1_{\alpha(sp-)}\rangle$ . We can now generalize this procedure to handle the interactions between several mutually orthogonal discrete zero phonon levels and a flat continuum with one LO phonon: each discrete level is coupled to only one particular linear combination of each continuum. So if we have  $N$  discrete levels and  $M$  continuums, we need only to consider  $N \times (M + 1)$  levels. In the present case, we have  $N=2$  ( $|p+, 0\rangle$  and  $|p-, 0\rangle$ ) and  $M=1$  ( $|s, 1\rangle$ ). We therefore expect to find four polaron levels. In this basis, the polaron wavefunction is written:

$$|\Psi\rangle = C_{p+}|p+, 0\rangle + C_{p-}|p-, 0\rangle + C_{sp+}|s, 1_{\alpha(sp+)}\rangle + C_{sp-}|s, 1_{\alpha(sp-)}\rangle \quad (\text{A4})$$

where  $|1_{\alpha(sp-)}\rangle$  is given in eqn. A2 and  $|1_{\alpha(sp+)}\rangle$  is obtained in a similar way. The corresponding eigenvalue equation is

$$\begin{pmatrix} \tilde{\varepsilon}_{s1} - E & v_{eff} & 0 & 0 \\ v_{eff} & \tilde{\varepsilon}_{p+0} - E & 0 & \delta_p \\ 0 & 0 & \tilde{\varepsilon}_{s1} - E & v_{eff} \\ 0 & \delta_p & v_{eff} & \tilde{\varepsilon}_{p-0} - E \end{pmatrix} \begin{pmatrix} C_{sp+} \\ C_{p+} \\ C_{sp-} \\ C_{p-} \end{pmatrix} = \vec{0} \quad (\text{A5})$$

where  $\delta_p$  is the anisotropy term that mixes the 0-phonon states of  $p$  symmetry and

$$\tilde{\varepsilon}_{s1} = E_s(B) + \hbar\omega_{LO} - \frac{\sum_{\mathbf{q}} |V_{ss}(\mathbf{q})|^2}{\hbar\omega_{LO}}, \quad (\text{A6})$$

$$\tilde{\varepsilon}_{p\pm 0} = E_{p\pm 0}(B) - \frac{\sum_{\mathbf{q}} |V_{pp}(\mathbf{q})|^2}{\hbar\omega_{LO}}, \quad (\text{A7})$$

$$v_{eff} = \sqrt{\sum_{\mathbf{q}} |V_{sp}(\mathbf{q})|^2}, \quad (\text{A8})$$

$$V_{ij}(\mathbf{q}) = \langle i|V(\mathbf{q})|j\rangle. \quad (\text{A9})$$

$E_j(B)$  is the  $B$ -dependent energy of the 0-phonon electronic level  $|j\rangle$ , which contains both a diamagnetic ( $\sim B^2$ ) and Zeeman ( $\sim B$ ) term. The last term in  $\tilde{\varepsilon}$  is a second order perturbation correction resulting from the interaction of  $|s, 0\rangle$  and  $|s, 2\rangle$  with  $|s, 1\rangle$  and  $|p\pm, 0\rangle$  with  $|p\pm, 1\rangle$ .

Note that a dot with cylindrical symmetry ( $\delta_p = 0$ ) has two independent sets of polaron levels, whose field dispersions are obtained by solving

$$(\tilde{\varepsilon}_{s1} - E)(\tilde{\varepsilon}_{p+0} - E) = v_{eff}^2 \quad (\text{A10})$$

or

$$(\tilde{\varepsilon}_{s1} - E)(\tilde{\varepsilon}_{p-0} - E) = v_{eff}^2. \quad (\text{A11})$$

Also note that in the absence of Fröhlich coupling ( $V_{ij} = 0$ ), eqn. A5 leads to two dispersion curves for the  $|p\pm, 0\rangle$  states, solutions of

$$[E_{p+0}(B) - E][E_{p-0}(B) - E] = |\delta_p|^2 \quad (\text{A12})$$

which we see in Fig. 4(a) in dashed lines.

In the general case, the discrete states are at the same time coupled to each other and to the continuum states. However, since the anisotropy term is weak in our samples ( $\delta_p \simeq 0.9\text{meV}$ ), the resulting polarons are roughly described in terms of the coupling of  $|s, 1_{\alpha(sp-)}\rangle$  with  $|p-, 0\rangle$  and  $|s, 1_{\alpha(sp+)}\rangle$  with  $|p+, 0\rangle$ .

The optical absorptions detected in our measurements (see Fig. 2) involve the excitation of the hole in the quantum dot from the ground state  $|s, 0\rangle$  towards the set of four polaron levels  $|\Psi\rangle$  resulting from the diagonalization of the  $4 \times 4$  matrix in eqn. A5. For light polarized in the QD layer plane the oscillator strength for each transition is proportional to

$$OS_{|\Psi\rangle} = |(C_{p+} + C_{p-})\epsilon_{[110]} + (C_{p+} - C_{p-})\epsilon_{[1\bar{1}0]}|^2, \quad (\text{A13})$$

where  $\epsilon$  is the in-plane polarization direction of the electromagnetic wave. We show in Fig. 6 the field dependence of the oscillator strength for the two low-lying polaron levels for both  $[110]$  and  $[1\bar{1}0]$  polarizations.

- 
- <sup>1</sup> S. Hameau, J.N. Isaia, Y. Guldner, E. Deleporte, O. Verzelen, R. Ferreira, G. Bastard, J. Zeman, and J.M. Gérard, Phys. Rev. B **65**, 085316 (2002).
- <sup>2</sup> D. Sarkar, H.P. van der Meulen, J.M. Calleja, J.M. Becker, R.J. Haug, and K. Pierz Phys. Rev. B **71**, 081302(R) (2005).
- <sup>3</sup> P.A. Knipp, T.L. Reinecke, A. Lorke, M. Fricke, and P.M. Petroff, Phys. Rev. B **56**, 1516 (1997).
- <sup>4</sup> S. Hameau, Y. Guldner, O. Verzelen, R. Ferreira, G. Bastard, J. Zeman, A. Lemaître, and J.M. Gérard, Phys. Rev. Lett. **83**, 4152 (1999).
- <sup>5</sup> O. Verzelen, R. Ferreira, and G. Bastard, Phys. Rev. B **62**, R4809 (2000).
- <sup>6</sup> T. Inoshita and H. Sakaki, Phys. Rev. B **56**, R4355 (1997).
- <sup>7</sup> X.Q. Li and Y. Arakawa, Phys. Rev. B **57**, 12285 (1998).
- <sup>8</sup> L. Goldstein, F. Glas, J.Y. Marzin, M.N. Charasse, and G. Leroux, Appl. Phys. Lett. **47**, 1099 (1985).
- <sup>9</sup> M. Fricke, A. Lorke, J.P. Kotthaus, G. Medeiros-Ribeiro, and P.M. Petroff, Europhys. Lett. **36**, 197 (1996).
- <sup>10</sup> Y. Hasegawa, H. Kiyama, Q.K. Xue, and T. Sakurai, Appl. Phys. Lett. **72**, 2265 (1998).
- <sup>11</sup> O. Stier, *Electronic and Optical Properties of Quantum Dots and Wires* (Wissenschaft und Technik Verlag).

- <sup>12</sup> G. Bester, S. Nair, and A. Zunger, Phys. Rev. B **67**,161306(R) (2003).
- <sup>13</sup> R. Ferreira, and G. Bastard, Appl. Phys. Lett. **74**, 2818 (1999).
- <sup>14</sup> R. Heitz, M. Veit, N.N. Ledentsov, A. Hoffmann, D. Bimberg, V.M. Ustinov, P.S. Kop'ev, and Zh.I. Alferov, Phys. Rev. B **56**, 10 435 (1997).